Impact of High PV Penetration on Voltage Stability

Jeremy Till[1], Shutang You[1], Yilu Liu[1,2], Pengwei Du[3]
University of Tennessee[1], Oak Ridge National Laboratory[2], Electric Reliability Council of Texas[3]
jatill42@students.tntech.edu, syou3@utk.edu; liu@utk.edu; Pengwei.Du@ercot.com

***Abstract*—Photovoltaics (PV) are becoming increasingly relevant in modern power systems. With this increase also comes reliability concerns as photovoltaics behave differently than conventional generators. One reliability concern is voltage stability. In this paper, voltage stability of the Austin area in the Electric Reliability Council of Texas (ERCOT) system is studied using dynamic models with varying levels of photovoltaic penetration. The base case is set at 0% renewable penetration. Additional cases include 15% wind penetration and up to 65% photovoltaic penetration. The study results show that voltage/var control capacity is critical to voltage stability, which PV lacks. Voltage regulation of photovoltaics may cause over-voltage and voltage collapse may be more abrupt under high regional photovoltaic penetration.**

Keywords—Voltage Stability, PV, Electric Reliability Council of Texas (ERCOT)

I. INTRODUCTION

Photovoltaics (PV) is increasingly popular. With the rise in PV, multiple reliability concerns arises for power grids with high PV penetration, including frequency stability [1, 2], oscillations [3, 4], transient angle stability [5, 6], and voltage stability [7, 8].

Voltage stability is the capability of power systems to maintain bus voltages at an acceptable range after a contingency or load change. Voltage usually collapses when the system is heavily loaded and cannot supply reactive power to maintain bus voltage [9-12]. There is evidence that voltage stability is directly impaired by an increase in PV generation based on power flow analysis [8, 13-16]. Studies have shown that PV poses risks due to unforeseen weather conditions leading to sudden decreases in generation. One study proposed that emergency battery energy storage could be utilized to maintain the grid under such failures [17]. The limited reactive power regulation capability of PV has also been discussed as a significant factor. Utilizing large-capacity inverters and reactive power resources to provide greater reactive power flexibility is an expensive but simple solution [17, 18]. In another study, PV penetration below 40% did not significantly impact the system in a modified IEEE 13 bus test system [7]. It has been shown that PV penetration on a small scale can increase voltage stability if PV can reduce long-distance power transfer [19] and that dispersed PV generators could have meaningfully less impact on voltage stability than PV farms [18]. Additional research regarding penetration levels in a system between 0-16% has shown that the voltage magnitude is reduced as penetration increases and is expected to continue to decrease above 16% [19].

This paper explores the impact of higher penetration levels on the voltage stability of the Electric Reliability Council of Texas (ERCOT) system. The voltage and reactive power control of PV are directly modeled in voltage stability study. In the studied scenarios, PV penetration ranges from 0-65% with an additional 15% wind generation for a total of 80% renewable penetration.

Section II provides a qualitative analysis on the impact mechanism of PV on voltage stability. Section III of this paper outlines the model for PV generation and the different renewable cases in this study. Section IV analyzes the voltage stability in the Austin region of the ERCOT system. Section V gives the conclusions.

II. QUALITATIVE ANALYSIS ON THE IMPACT OF PV ON VOLTAGE STABILITY

Voltage stability will be impacted by the displacement of synchronous generators with PV because of unique characteristics in voltage and reactive power control of PV generation. The impact of PV on voltage stability can be studied using the equations derived from a simple radial system, as shown in Figure 1.

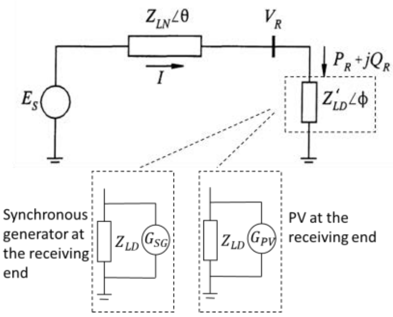

Figure 1. A simple radial system diagram

For a simple radial system [9], the receiving end voltage is shown in (1).

$$V_R = \frac{1}{\sqrt{F}}\frac{Z'_{LD}}{Z_{LN}}E_S \quad (1)$$

The receiving end power is shown in (2).

$$P_R = \frac{Z'_{LD}}{F}\left(\frac{E_S}{Z_{LN}}\right)^2 cos\phi \quad (2)$$

where

$$F = 1 + \left(\frac{Z'_{LD}}{Z_{LN}}\right)^2 + 2\left(\frac{Z'_{LD}}{Z_{LN}}\right)\cos\left(\theta - \phi\right) \quad (3)$$

This work is funded in whole by the U.S. Department of Energy Solar Energy Technologies Office, under Award Number 30844.

This work made use of Engineering Research Center shared facilities supported by the Engineering Research Center Program of the National Science Foundation and the Department of Energy under NSF Award Number EEC-1041877 and the CURENT Industry Partnership Program.

978-1-7281-4547-1/20/$31.00 ©2020 IEEE

Due to the limited converter current capacity of PV, its reactive power capacity is usually smaller compared with that of a synchronous generator, especially when PV's real power output is close to the rated value. Therefore, if the receiving end has a higher PV penetration rate and PV's reactive power limit is reached, reactive power demand could be larger as load increases. Thus, the power factor of the equivalent load impedance ($cos\phi$) will further lag. Based on (1) and (3), the further lag power factor at the receiving end will lead to a smaller margin of voltage stability.

III. THE ERCOT SYSTEM AND PV MODEL

The ERCOT system consists of over 40 thousand miles of transmission lines and more than 700 generators, serving 24 million customers (or 85% population) in the Texas state. The peak load of ERCOT is around 70 GW. Its peak load usually happens in summer, when air condition power takes a substantial portion of the total demand. The ERCOT system model represents the ERCOT system ranging from generation, transmission to distribution. Generators, exciters, and governors' dynamics are modeled in details. As a generic approach, real power of loads are modeled as constant current loads and reactive power of loads as constant impedance loads. The geographic locations of the Austin area are shown in Figure 2

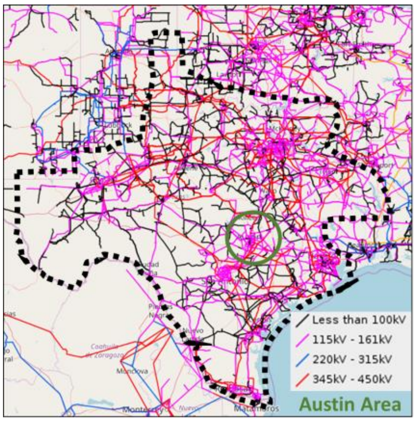

Figure 2. ERCOT system model [22]

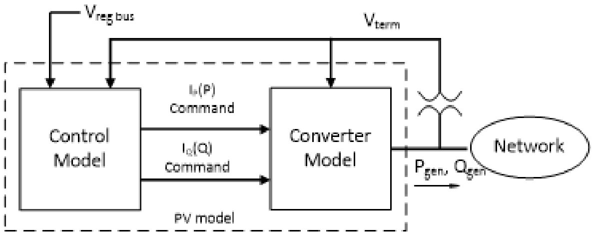

Figure 3. PV dynamic model connectivity [23]

The dynamic PV models used in this study were created by General Electric representing utility-scale PV farms. For power flow, the equivalent reactance for current injection is set to a large number and the internal resistance is set to zero to model power electronics interfaced generation [3, 20]. The GEPVG (the PV inverter model developed by GE in PSS/e) and GEPVE (the PV inverter electrical controller model developed by GE in PSS/e) models were used for the inverter and control models, as shown in Figure 3. The control sends commands of active and reactive power outputs, which are executed by PV inverters [21]. Parameters for the PV model can be found in the appendix.

Four potential scenarios were developed for dynamic simulations as shown in Table I and Figure 4. Transmission power flow is kept unchanged for all simulated scenarios and synchronous units are displaced by PV farms to avoid other factors' impacts. For the 40% renewable scenario, renewable penetration (wind + PV) has already reached 100% in West ERCOT due to high wind penetration in this region. Therefore, for the remaining two scenarios (60% and 80%), PV penetration increases are mainly located in the north and south of Texas due to the saturation of renewable penetration in the west.

IV. AUSTIN POWER-VOLTAGE ANALYSIS

Voltage instability may arise due to many reasons including but not limited to: load increases, device reaching power ratings, transformer tap changes, and the recovery dynamics of loads. To quantify the voltage stability margin, load was incrementally and uniformly changed in the Austin region until voltage collapsed. Simulations were performed in PSS/e. The power-voltage relationship was analyzed by plotting the voltage at the buses over the power demand of the Austin region.

TABLE I. SIMULATION SCENARIOS

Scenario	Renewable Penetration Level		
	PV	***Wind***	***Total***
#0	0%	0%	0%
#1	5%	15%	20%
#2	25%	15%	40%
#3	45%	15%	60%
#4	65%	15%	80%

A. Base Case

Importing a large amount of power, Austin is located in the southern area of ERCOT. A dynamic simulation was initialized under a summer peak-load case. The resulting power-voltage curve is shown in Figure 5.

The base case was initialized at 2,600 MW load. The voltage stability margin in the Austin region is 5,500 MW without contingency applied (the margin may be further constrained by N-1 or N-2 analysis, the loss of one or two large transmission elements simultaneously, respectively). To visualize the system voltage as a whole, a visualization tool was created to animate the voltage collapse by mapping out bus voltage data onto the Texas territory. Figure 6 is a still image at the point of voltage collapse in the base case. Figure 5 and Figure 6 validated that the voltage stability issue in the study case is located in the Austin region.

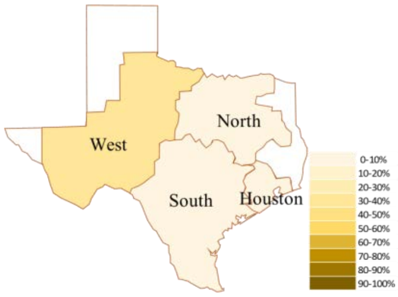

(a) 20% renewable (15% WT + 5% PV)

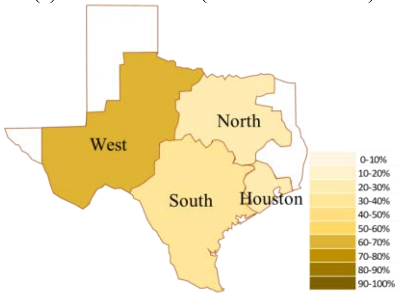

(b) 40% renewable (15% WT + 25% PV)

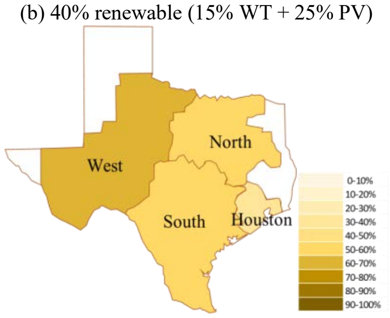

(c) 60% renewable (15% WT + 45% PV)

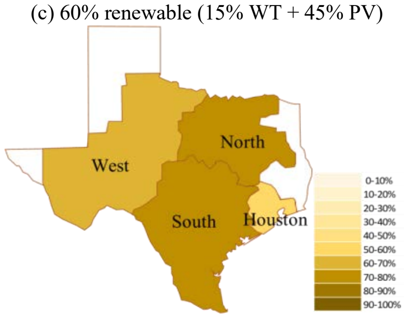

(d) 80% renewable (15% WT + 65% PV)

Figure 4. PV penetration range for each simulation case in ERCOT [24]

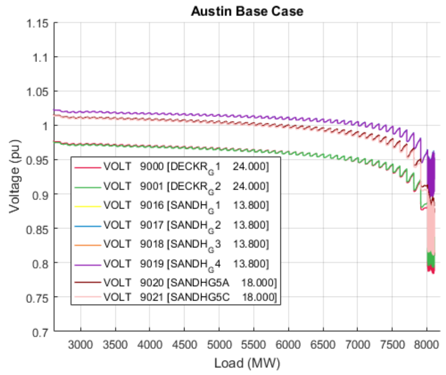

Figure 5. Power-voltage curve of base case simulation in Austin

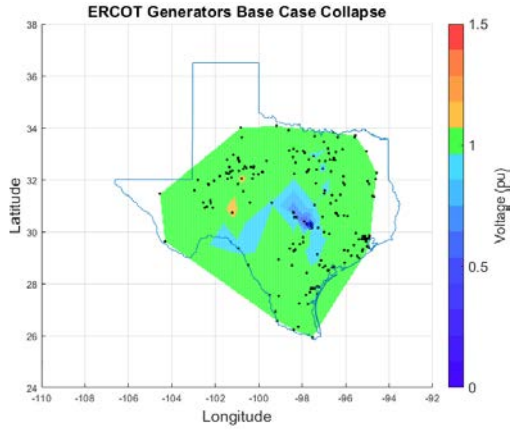

Figure 6. The voltage collapse snapshot of the ERCOT base case

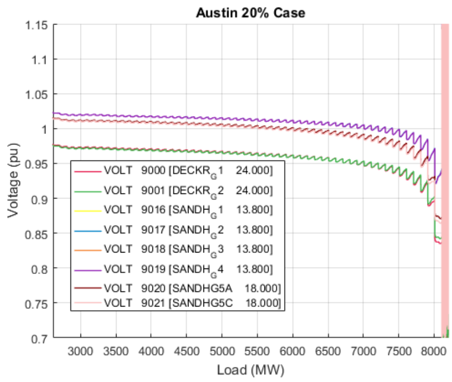

Figure 7. Power-voltage curves of 20% case simulation in Austin

B. High PV Cases

The simulation result for the 20% case is shown in Figure 7. In the 20% renewable (15% wind + 5% PV) case, most renewables are wind turbines mostly located in West ERCOT. As the 20% renewable case does not introduce PV penetration to the Austin region, the voltage stability of the Austin region is unaffected by the increase in PV in the other areas.

In the 40% case, two synchronous generators were replaced with centralized PV farms in the Austin region. The resulting power-voltage curve is shown in Figure 8.

Multiple effects of PV penetration are visible in the 40% case. The system stability margin is approximately 7,600 MW, 500 MW smaller than the 20% cases. In addition, it can be noticed that the voltage profile of a PV integration bus has a peak as load increases. This peak in voltage profile of the PV bus is caused by the voltage control of PV. As load increases, the voltage at the transmission level decreases. Conventional generators maintain generator terminal voltage as constants while PV farms will increase reactive power generation in order to maintain voltage levels at voltage-reference buses. After crossing the reference point, the voltage starts to decrease because the PV reactive power output cannot further increase due to the converter current limit of PV. After that, the PV generator becomes a PQ bus and can no longer maintain the voltage level at the remote voltage-reference bus.

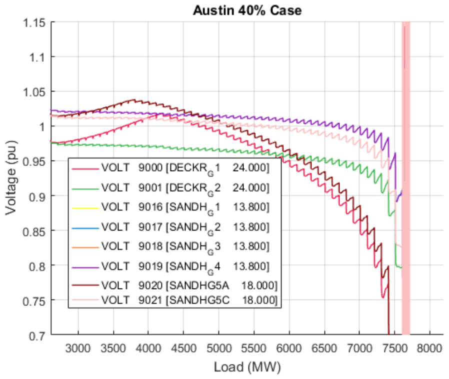

Figure 8. Power-voltage curves of 40% case simulation in Austin

Furthermore, the 60% case shows a consistent change in voltage stability margin, as shown in Figure 9. The system stability margin is approximately 7,000 MW, 500 MW less again than the 40% case. Comparing with the 40% renewable case, it can be seen that the peak voltage points for PV buses moved to the right. The reason is that reactive power for voltage regulation is shared among more PV generation in Austin in the 60% renewable case, so that the load levels at which PV converters reach their limits are higher than those of the 40% renewable case.

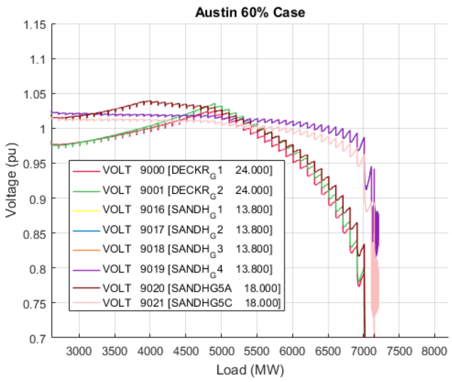

Figure 9. Power-voltage curves of 60% case simulation in Austin

The case with the least stability margin is 80% penetration, in which all synchronous generators in the Austin region are displaced with PV, and is visible in Figure 10.

In the 80% case, the system stability margin is smaller than the 60% case, but there is not as great of a difference as those between previous cases due to the disproportion of PV penetration growth in Austin (smaller than 20% increase in regional PV penetration) and the entire ERCOT (20% increase). Moreover, the voltage peaks of a few buses are significantly above normal bus voltage due to reactive current injection of PV to regulate the voltage of reference buses. With more PV generation in the Austin area, the voltage is more strictly regulated by converter current limits of PV power plants. As the load increases, converter currents successively hit limits and the voltage decline begins to accelerate. The highest PV penetration and the constrained reactive power support result in the smallest voltage stability margin for the 80% renewable case.

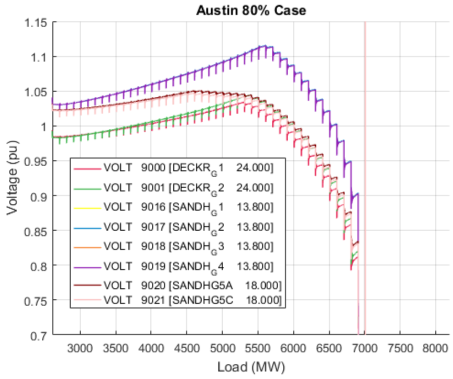

Figure 10. Power-voltage curves of 80% case simulation in Austin

These power-voltage curves are combined on the same axis in Figure 11. It is clear that as PV penetration increases voltage stability margin becomes smaller, as listed in Table II. This result is consistent with the qualitative analysis in Section II.

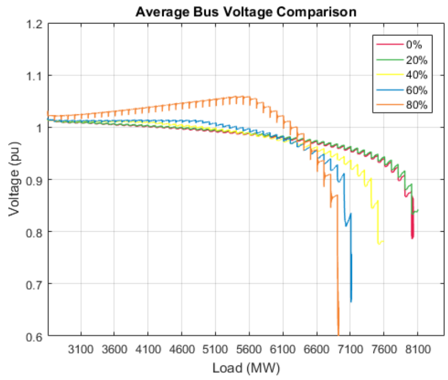

Figure 11. Average power-voltage curves of all case simulations in Austin

TABLE II. LOAD VALUES FOR ALL PV CASES IN AUSTIN

Scenario	*Renewable Percentage*	*Voltage Knee (MW)*	*Voltage Collapse (MW)*
#0	0%	2600	8100
#1	20%	2600	8100
#2	40%	3800	7600
#3	60%	4000	7100
#4	80%	5500	6900

V. CONCLUSIONS

In this paper, the effect of up to 65% PV penetration on voltage stability in the ERCOT system was studied using detailed dynamic models. It was demonstrated that within the PV converter capability, the reference transmission bus voltage can be strictly regulated compared with synchronous generators equipped with exciters. Despite that, overvoltage may occur at the point of PV connection due to reactive current injection. When the PV converter capacity is exhausted, the voltage at the reference point begins to decrease dramatically. The voltage stability is closely related to the converter capacity and the reactive power capacity of PV generation. Under existing settings of PV voltage/var control and converter capacity selection, the voltage stability will be substantially impaired by the increase of PV penetration. Foreseeing these voltage problems, installing capacitors, static var compensators and static synchronous compensators are likely to be mitigation tactics, which will be studied in future work.

ACKNOWLEDGMENT

The authors would like to thank Dr. Tassos Golnas, Dr. Guohui Yuan and Dr. Rebecca Hott, from the U.S. Department of Energy Solar Energy Technologies Office (SETO) for their guidance and support.

APPENDIX

TABLE III. PV CONVERTER MODEL 'GEPVG' PARAMETERS [16]

Parameter	*Value*
Xeq-equivalent reactance for current injection	99999
VHVRCR2- HVRCR voltage 2	1.2
CURHVRCR2- Max. reactive current at VHVRCR2	2.0
RIp_LVPL-Rate of active current change	5.0
T_LVPL-Voltage sensor for LVPL	0.02
LVPL voltage 1	0
LVPL power 1	0
LVPL voltage 2	0.5
LVPL power 2	0.167
LVPL voltage 3	0.9
LVPL power 3	0.98
XLVPL	0

TABLE IV. PV ELECTRICAL CONTROLLER 'GEPVE' PARAMETERS [16]

Parameter	*Value*
Tfv - V-regulator filter	0.15
Kpv - V-regulator proportional gain	18.0
Kiv - V-regulator integrator gain	5.0
Rc - line drop compensation resistance	0
Xc - line drop compensation reactance	0
QMX - V-regulator max limit	1.0
QMN - V-regulator min limit	-1.0
IPMAX - Max active current limit	1.12
TRV - V-sensor	0.02
KQi - MVAR/Volt gain	0.1
VMINCL	0.88
VMAXCL	1.15
KVi - Volt/MVAR gain	120
XIQmin - min. limit for Eq'cmd	0.55
XIQmax - max. limit for Eq'cmd	1.55
Tv - Lag time constant in WindVar controller	0.05
Tp - Pelec filter in fast PF controller	0.05
Fn - A portion of on-line PV converters	1.0
ImaxTD - Converter current limit	1.12
Iphl - Hard active current limit	1.12
Iqhl - Hard reactive current limit	1.12
TIpqd - Reactive droop time constant	5.0
Kqd - Reactive droop gain	0.0
Xqd - Reactive droop synthesizing Impedance	0.0
Vermx - Reactive power control maximum error signal	0.01
Vermn - Reactive power control minimum error signal	-0.01
Vfrz - Reactive power control freeze voltage	0.7
PFAFLG: (=1 if PF fast control enabled)	0
VARFLG: (=1 if Qord is provided by SolarVar)	1
PQFLAG: (=1 for P priority, =0 for Q priority)	1

REFERENCES

[1] S. You *et al.*, "Non-Invasive Identification of Inertia Distribution Change in High Renewable Systems Using Distribution Level PMU," *IEEE Transactions on Power Systems,* vol. 33, no. 1, pp. 1110-1112, 2018.

[2] J. Tan, Y. Zhang, S. You, Y. Liu, and Y. Liu, "Frequency Response Study of U.S. Western Interconnection under Extra-High Photovoltaic Generation Penetrations," in *Power & Energy Society General Meeting, 2018 IEEE*, 2018, pp. 1-5: IEEE.

[3] S. You *et al.*, "Impact of High PV Penetration on the Inter-Area Oscillations in the US Eastern Interconnection," *IEEE Access,* vol. 5, pp. 4361-4369, 2017.

[4] J. Quintero, V. Vittal, G. T. Heydt, and H. Zhang, "The impact of increased penetration of converter control-based generators on power system modes of oscillation," *IEEE Transactions on Power Systems,* vol. 29, no. 5, pp. 2248-2256, 2014.

[5] P. G. Bueno, J. C. Hernández, and F. J. Ruiz-Rodriguez, "Stability assessment for transmission systems with large utility-scale photovoltaic units," *IET Renewable Power Generation,* vol. 10, no. 5, pp. 584-597, 2016.

[6] S. Eftekharnejad, "The Impact of increased penetration of photovoltaic generation on smart grids," Arizona State University, 2012.

[7] R. Yan and T. K. Saha, "Investigation of voltage stability for residential customers due to high photovoltaic penetrations," *IEEE transactions on power systems,* vol. 27, no. 2, pp. 651-662, 2012.

[8] D. Q. Hung, N. Mithulananthan, and R. Bansal, "Integration of PV and BES units in commercial distribution systems considering energy loss and voltage stability," *Applied Energy,* vol. 113, pp. 1162-1170, 2014.

[9] P. Kundur, N. J. Balu, and M. G. Lauby, *Power system stability and control*. McGraw-hill New York, 1994.

[10] B. H. Chowdhury and C. W. Taylor, "Voltage stability analysis: VQ power flow simulation versus dynamic simulation," *IEEE Transactions on Power Systems,* vol. 15, no. 4, pp. 1354-1359, 2000.

[11] Y. Kataoka and Y. Shinoda, "Voltage stability limit of electric power systems with generator reactive power constraints considered," *IEEE Transactions on Power Systems,* vol. 20, no. 2, pp. 951-962, 2005.

[12] H. Kwatny, A. Pasrija, and L. Bahar, "Static bifurcations in electric power networks: Loss of steady-state stability and voltage collapse," *IEEE Transactions on Circuits and Systems,* vol. 33, no. 10, pp. 981-991, 1986.

[13] H. Li, Y. Xu, S. Adhikari, D. T. Rizy, F. Li, and P. Irminger, "Real and reactive power control of a three-phase single-stage PV system and PV voltage stability," in *Power and Energy Society General Meeting, 2012 IEEE*, 2012, pp. 1-8: IEEE.

[14] E. Demirok, D. Sera, R. Teodorescu, P. Rodriguez, and U. Borup, "Clustered PV inverters in LV networks: An overview of impacts and comparison of voltage control strategies," in *Electrical Power & Energy Conference (EPEC), 2009 IEEE*, 2009, pp. 1-6: IEEE.

[15] J. Hernández, A. Medina, and F. Jurado, "Optimal allocation and sizing for profitability and voltage enhancement of PV systems on feeders," *Renewable Energy,* vol. 32, no. 10, pp. 1768-1789, 2007.

[16] K. Le Dinh and Y. Hayashi, "Coordinated BESS control for improving voltage stability of a PV-supplied microgrid," in *Power Engineering Conference (UPEC), 2013 48th International Universities'*, 2013, pp. 1-6: IEEE.

[17] K. Kawabe and K. Tanaka, "Impact of dynamic behavior of photovoltaic power generation systems on short-term voltage stability," *IEEE Transactions on Power Systems,* vol. 30, no. 6, pp. 3416-3424, 2015.

[18] B. Tamimi, C. Cañizares, and K. Bhattacharya, "System stability impact of large-scale and distributed solar photovoltaic generation: The case of Ontario, Canada," *IEEE transactions on sustainable energy,* vol. 4, no. 3, pp. 680-688, 2013.

[19] R. Shah, N. Mithulananthan, R. Bansal, and V. Ramachandaramurthy, "A review of key power system stability challenges for large-scale PV integration," *Renewable and Sustainable Energy Reviews,* vol. 41, pp. 1423-1436, 2015.

[20] S. You, Y. Liu, M. Gonzales, X. Zhang, and Y. Liu, "U.S. Eastern Interconnection (EI) Electromechanical Wave Propagation and the Impact of High PV Penetration on Its Speed," presented at the 2018 IEEE PES T&D Conference & Exposition, 2018.

[21] K. Clark, N. W. Miller, and R. Walling, "Modeling of GE solar photovoltaic plants for grid studies," *General Electric International. Inc, Schenectady, NY,* vol. 12345, 2010

[22] V. Koritarov, J. Kuiper, K. Hlava, A. Orr, and K. Rollins, "Energy Zones Study: A Comprehensive Web-Based Mapping Tool to Identify and Analyze Clean Energy Zones in the Eastern Interconnection," Argonne National Laboratory (ANL)2013.

[23] S. You *et al.*, "Impact of high PV penetration on US eastern interconnection frequency response," in *Power & Energy Society General Meeting, 2017 IEEE*, 2017, pp. 1-5: IEEE.

[24] Y. Liu, S. You, J. Tan, Y. Zhang, and Y. Liu, "Frequency Response Assessment and Enhancement of the US Power Grids towards Extra-High Photovoltaic Generation Penetrations–an Industry Perspective," *IEEE Transactions on Power Systems,* 2018.